AMERICAN SOCIETY FOR MICROBIOLOGY | Applied and Environmental Microbiology®

ENVIRONMENTAL MICROBIOLOGY

Interspecies Chemical Signaling in a Methane-Oxidizing Bacterial Community

Aaron W. Puri,[a]* Darren Liu,[a] Amy L. Schaefer,[b] Zheng Yu,[a] Mitchell W. Pesesky,[a] E. Peter Greenberg,[b] Mary E. Lidstrom[a,b]

[a]Department of Chemical Engineering, University of Washington, Seattle, Washington, USA
[b]Department of Microbiology, University of Washington, Seattle, Washington, USA

ABSTRACT Multiple species of bacteria oxidize methane in the environment after it is produced by anaerobic ecosystems. These organisms provide reduced carbon substrates for species that cannot oxidize methane themselves, thereby serving a key role in these niches while also sequestering this potent greenhouse gas before it enters the atmosphere. Deciphering the molecular details of how methane-oxidizing bacteria interact in the environment enables us to understand an important aspect that shapes the structures and functions of these communities. Here we show that many members of the *Methylomonas* genus possess a LuxR-type acyl-homoserine lactone (acyl-HSL) receptor/transcription factor that is highly homologous to MbaR from the quorum-sensing (QS) system of *Methylobacter tundripaludum*, another methane oxidizer that has been isolated from the same environment. We reconstitute this detection system in *Escherichia coli* and use mutant and transcriptomic analysis to show that the receptor/transcription factor from *Methylomonas* sp. strain LW13 is active and alters LW13 gene expression in response to the acyl-HSL produced by *M. tundripaludum*. These findings provide a molecular mechanism for how two species of bacteria that may compete for resources in the environment can interact in a specific manner through a chemical signal.

IMPORTANCE Methanotrophs are bacteria that sequester methane, a significant greenhouse gas, and thereby perform an important ecosystem function. Understanding the mechanisms by which these organisms interact in the environment may ultimately allow us to manipulate and to optimize this activity. Here we show that members of a genus of methane-oxidizing bacteria can be influenced by a chemical signal produced by a possibly competing species. This provides insight into how gene expression can be controlled in these bacterial communities via an exogenous chemical signal.

KEYWORDS acyl-homoserine lactone, LuxR solo, methane, methanotroph, orphan LuxR, quorum sensing, sociomicrobiology

Methane-oxidizing bacterial communities sequester this potent greenhouse gas after it is produced by anaerobic ecosystems (1, 2). The aerobic methanotrophs involved in this process have been extensively studied in the sediment communities in Lake Washington (Seattle, WA, USA) (3–6). Evidence shows that several methane-oxidizing bacterial species are present in these environments and compete under different compositions of oxygen and methane gas (5–8). These species also provide a carbon and energy source for organisms that cannot oxidize methane themselves (9–11), thereby serving a foundational role in these ecosystems.

We previously identified and characterized a quorum-sensing (QS) system in *Methylobacter tundripaludum* (12), a dominant member of enrichments of these methane-oxidizing sediment communities (5, 13). QS is a chemical signaling mechanism that enables bacteria to control gene expression in a cell-density-dependent manner (re-

Citation Puri AW, Liu D, Schaefer AL, Yu Z, Pesesky MW, Greenberg EP, Lidstrom ME. 2019. Interspecies chemical signaling in a methane-oxidizing bacterial community. Appl Environ Microbiol 85:e02702-18. https://doi.org/10.1128/AEM.02702-18.

Editor Rebecca E. Parales, University of California, Davis

Address correspondence to Aaron W. Puri, a.puri@utah.edu.

* Present address: Aaron W. Puri, Department of Chemistry and the Henry Eyring Center for Cell and Genome Science, University of Utah, Salt Lake City, Utah, USA.

Received 7 November 2018
Accepted 29 January 2019
Accepted manuscript posted online 1 February 2019
Published 22 March 2019

viewed in references 14 and 15). One well-studied form of QS uses as chemical signals acyl-homoserine lactones (acyl-HSLs), which are produced by LuxI-type acyl-HSL synthases and are detected by LuxR-type receptors that also serve as transcription factors to regulate gene expression. In *M. tundripaludum*, the acyl-HSL synthase MbaI produces *N*-3-hydroxydecanoyl-L-homoserine lactone (3-OH-C_{10}-HSL), which is detected by the transcription factor/receptor MbaR (12). MbaR in turn activates a biosynthetic gene cluster that produces the specialized metabolite tundrenone (16).

Although QS was first described as an intraspecies communication system, there is precedence for its use in interspecies signaling as well. Genes encoding LuxR-type receptors in many bacterial genomes are found with no cognate signal synthase and are known as orphans or solos (17, 18). These receptors can be found in species that do not produce any acyl-HSL signals, such as SdiA in *Escherichia coli* and *Salmonella enterica*, which regulates adhesion and resistance to the innate immune system in *S. enterica* in response to exogenous acyl-HSLs (19). Orphan receptors can also be found in bacteria that possess *luxI/luxR*-type pairs in their genomes, such as QscR in *Pseudomonas aeruginosa*, which controls acyl-HSL and virulence factor production in response to both endogenously and exogenously produced signals (20, 21). Bioinformatic surveys (22–24) show that orphan LuxR-type receptors are widespread in bacterial genomes, which suggests that they could play a prominent role in interspecies chemical signaling. To date, however, relatively few of these systems have been characterized experimentally.

In this work, we identify an orphan QS receptor in the genome of many members of the methane-oxidizing genus *Methylomonas*, including strains isolated from the same environment as the QS-active *M. tundripaludum*. We show that the orphan receptor/transcription factor from *Methylomonas* species strain LW13 (13) is active in response to multiple acyl-HSL signals and controls transcription of a neighboring gene cluster that is partially conserved in all orphan-containing members of the *Methylomonas* genus. Finally, we demonstrate that this gene cluster is also transcribed during coculture with *M. tundripaludum* but this eavesdropping is not a dominant influence on the dynamics of competition between these two organisms when they are grown planktonically under methane gas in the laboratory. These results identify a molecular mechanism for interspecies chemical communication between two members of a methane-oxidizing bacterial community, an important ecological system.

RESULTS

Identification of an orphan QS receptor in LW13. We recently characterized a QS system used by the methane-oxidizing bacterium *M. tundripaludum* 21/22, a strain isolated from sediment from Lake Washington (Seattle, WA, USA). Many other bacterial isolates from the same environment have sequenced genomes (13, 25), and we hypothesized that other organisms that may compete for the same niche might be able to detect the QS signal produced by *M. tundripaludum*. We performed a BLAST search with the amino acid sequence of the *M. tundripaludum* LuxR-type receptor/transcription factor MbaR. *Methylomonas* species strain LW13 possesses an ortholog with 67% amino acid identity to MbaR, which we have named MmsR (Fig. 1A). The amino acid sequence of MmsR retains all of the residues conserved among LuxR-type transcription factors/receptors that bind acyl-HSLs (Fig. 1B) (26, 27).

We were unable to locate a cognate *luxI*-type acyl-HSL synthase gene in the LW13 genome, implicating MmsR as an orphan (or solo) LuxR-type receptor/transcription factor. However, the LW13 draft genome is made up of 42 scaffolds (13), suggesting that it may be missing several open reading frames (ORFs). We used nanopore long read sequencing to close the genome, resulting in one 5,233,521-bp circular chromosome (see Fig. S1 in the supplemental material). This revised genome sequence confirmed that the LW13 genome does not contain an acyl-HSL synthase gene, and it also provided genomic context for the region around *mmsR*, which was originally near the end of one of the scaffolds.

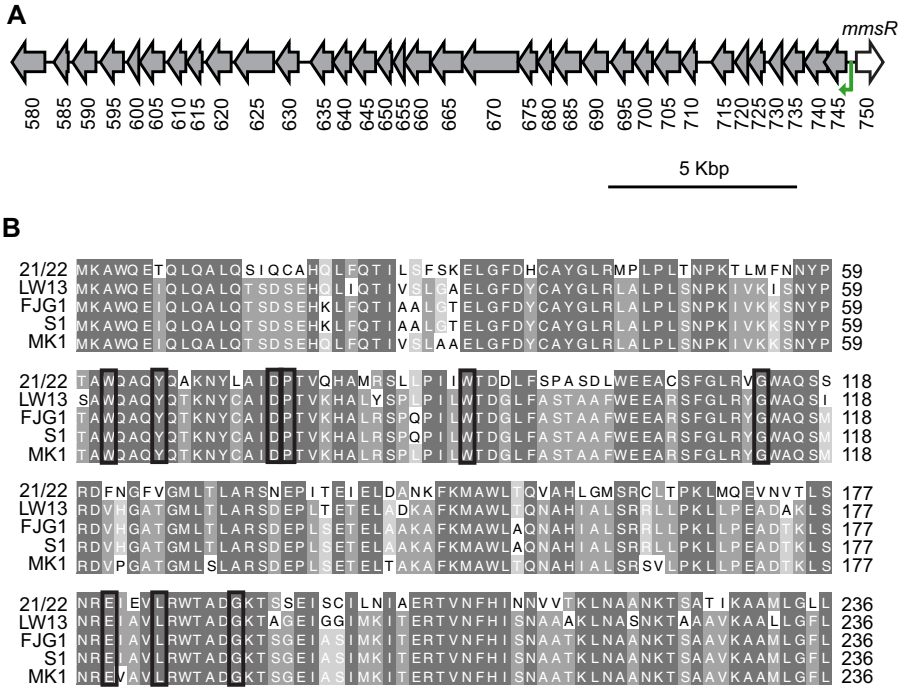

FIG 1 Orphan LuxR-type receptor/transcription factor in members of the *Methylomonas* genus. (A) LW13 genomic region containing the orphan receptor gene *mmsR* and the predicted MmsR binding site (green arrow) (also see Fig. 2A) upstream of a neighboring gene cluster. Locus tags listed below ORFs are preceded by U737_12 and correspond to the LW13 genome described in this work. (B) Amino acid sequence comparison of the LuxR-type receptor MbaR from *M. tundripaludum* 21/22 (IMG locus tag T451DRAFT_0820) and homologs from *Methylomonas* strains, including *Methylomonas* sp. strain LW13 (U737_12750), *Methylomonas denitrificans* FJG1 (IMG locus tag Ga0213656_112931), *Methylomonas methanica* S1/NCIMB 11130 (IMG locus tag Ga0133021_101333), and *Methylomonas* sp. strain MK1 (IMG locus tag G006DRAFT_0604). Black boxes indicate amino acids conserved in LuxR-type transcription factors/receptors that bind acyl-HSLs (26, 27).

When we analyzed published genomes, we discovered that many other *Methylomonas* strains also possess MmsR, including the type strain *Methylomonas methanica* S1/NCIMB 11130 (28), the well-studied organism *Methylomonas denitrificans* FJG1 (29), and another isolate from Lake Washington sediment, *Methylomonas* sp. strain MK1 (13) (Fig. 1; also see Fig. S2). Therefore, we sought to determine the function of MmsR.

MmsR responds to acyl-HSL signals via a neighboring binding site in the genome. In each *Methylomonas* genome that contains *mmsR*, it is neighbored by a cluster of genes downstream of a predicted LuxR-type transcription factor binding site ("*lux* box") (30, 31) (Fig. 1A and Fig. 2A). We hypothesized that the orphan receptor activates gene expression via this site upon acyl-HSL signal binding. To test this hypothesis experimentally, we constructed a two-plasmid *E. coli* reporter strain (P_{12745}-*gfp*) in which one plasmid expresses *mmsR* via its native promoter and the other contains the putative MmsR binding site upstream of gene U737_12745 fused to a green fluorescent protein (GFP) gene (*gfp*), as has been done for other QS systems (12, 32).

When we grew this reporter strain in the presence of an ethyl acetate extract of supernatant from wild-type *M. tundripaludum*, an approximately 5-fold increase in normalized green fluorescence was observed (Fig. 2B). Commercially available 3-OH-C_{10}-HSL, the QS signal produced by *M. tundripaludum*, also activated the reporter strain. To confirm that the acyl-HSL is the only factor produced by *M. tundripaludum* that activates the reporter strain, we also tested supernatant extract from an *M. tundripaludum* Δ*mbaI* strain that does not produce 3-OH-C_{10}-HSL (12), which resulted in no increase in normalized green fluorescence (Fig. S3).

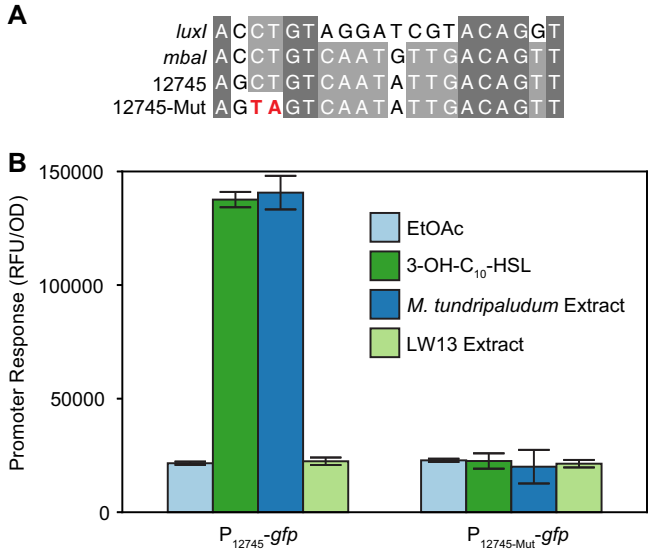

FIG 2 Direct MmsR activation of the promoter of the neighboring gene U737_12745 via a predicted binding site. (A) Comparison of the wild-type and mutated genes for the predicted MmsR binding site upstream of ORF U737_12745 with known *lux* boxes in the promoter sequences of *Vibrio fischeri luxI* and *M. tundripaludum mbaI*. (B) Response of an *E. coli* reporter strain containing *gfp* fused to the promoter region of ORF U737_12745, in addition to *mmsR* on a separate plasmid, to an acyl-HSL signal. EtOAc, ethyl acetate (solvent control); 3-OH-C_{10}-HSL, 10 nM commercially available signal; *M. tundripaludum* and LW13 extract, ethyl acetate extracts from the supernatants of stationary-phase cultures of *M. tundripaludum* and LW13, respectively. Data are the mean ± standard deviation of three cultures.

We also did not see an increase in fluorescence when supernatant extract from LW13 itself was tested (Fig. 2B), confirming that LW13 does not produce an acyl-HSL. We then constructed another version of the strain ($P_{12745mut}$-*gfp*), containing a mutation of CT to TA in the predicted MmsR binding site (Fig. 2A). This mutation resulted in a loss of responses to both *M. tundripaludum* supernatant extract and 3-OH-C_{10}-HSL (Fig. 2B). These results demonstrate that the orphan MmsR from LW13 is functional and this transcription factor can directly activate a gene downstream of an MmsR binding site in response to the acyl-HSL signal 3-OH-C_{10}-HSL.

MmsR has broader acyl-HSL specificity than MbaR in *E. coli* reporter assays. We tested the difference in acyl-HSL signal specificity of the orphan MmsR and the highly homologous MbaR from *M. tundripaludum*. We used a previously constructed reporter strain containing *mbaR* and the MbaR binding site (12) for comparison with the P_{12745}-*gfp* reporter strain, using several commercially available acyl-HSLs with different acyl chain lengths and/or substituents at the third carbon of the acyl chain. MbaR was most responsive to its cognate signal, 3-OH-C_{10}-HSL, but also was sensitive (saturation at $<$150 nM) to the other signals with a hydroxyl at the third carbon of the acyl chain (3-OH-C_8-HSL and 3-OH-C_{12}-HSL) tested in this assay (Fig. 3). MbaR showed very little response to the other signals, even at the maximum concentration tested (300 nM). In contrast, MmsR showed some response to all acyl-HSLs tested at a concentration of 50 nM in this assay. Among the panel of signals tested, MmsR also appeared most responsive to 3-OH-C_{10}-HSL. Together, these results show that the orphan transcription factor MmsR responds to a broader range of acyl-HSL signals than MbaR under the conditions tested.

MmsR activates the expression of a neighboring gene cluster in the LW13 genome in response to 3-OH-C_{10}-HSL. In order to determine which genes MmsR regulates in response to an acyl-HSL signal, we compared the transcriptome of exponentially growing LW13 cells in the presence versus the absence of 2 μM 3-OH-C_{10}-HSL. To assess whether any detected expression changes are not dependent on signal binding to MmsR, we constructed an unmarked, in-frame deletion of *mmsR* (Δ*mmsR*) and compared the transcriptome of that strain in the presence versus the absence of an acyl-HSL signal.

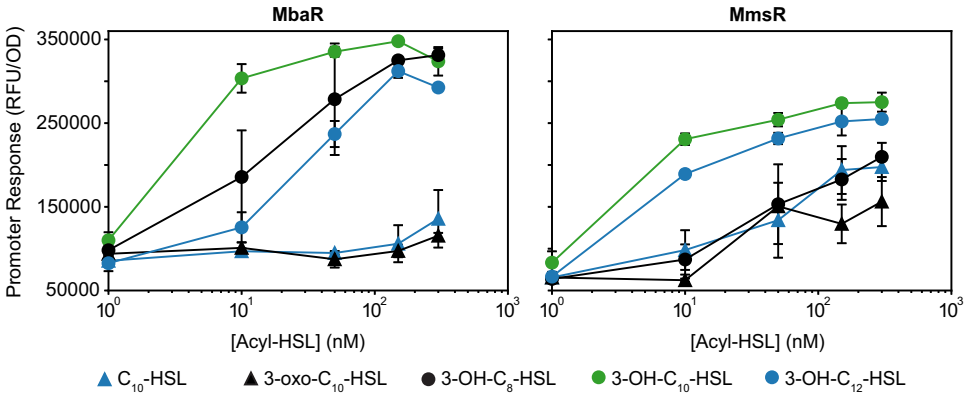

FIG 3 Broader acyl-HSL signal specificity of MmsR than MbaR. *E. coli* reporter strains assessing MbaR and MmsR activity were assayed with several commercially available acyl-HSL signals. Data are the mean and range of two cultures and are representative of two independent experiments.

The doubling time of the mutant was not significantly different from that of the wild-type LW13 strain, and there were no significant differences in the doubling times in the presence versus the absence of acyl-HSL for either strain (Table S1).

The neighboring cluster downstream of the identified MmsR binding site was the only group of genes found to be activated in the presence of acyl-HSL (Table 1). The

TABLE 1 Genes with increased expression in LW13 in the presence of 2 μM 3-OH-C_{10}-HSL, compared to the absence of an acyl-HSL signal or compared to the Δ*mmsR* strain also in the presence of an acyl-HSL signal[a]

		With vs without acyl-HSL		Wild type with acyl-HSL vs Δ*mmsR* with acyl-HSL	
Gene locus	Predicted product[b]	Fold change	Adjusted *P*	Fold change	Adjusted *P*
U737_12595	Hypothetical protein	1.6	1.0E−03	1.6	1.5E−04
U737_12600	Antibiotic biosynthesis monooxygenase	1.9	3.0E−08	1.8	1.5E−06
U737_12605	Glutathione *S*-transferase	1.9	4.3E−09	2.0	2.7E−10
U737_12610	Phosphotyrosine protein phosphatase	2.1	1.5E−11	2.1	1.5E−11
U737_12615	GFA family protein	2.4	1.6E−17	2.6	1.3E−19
U737_12620	Glutathione *S*-transferase family protein	2.2	7.9E−15	2.5	2.5E−19
U737_12625	α/β-Hydrolase	3.0	7.6E−26	3.2	4.0E−30
U737_12630	Hypothetical protein	3.4	9.8E−34	3.5	2.7E−34
U737_12635	PAP2 family protein	3.2	3.8E−32	3.6	1.6E−39
U737_12640	GNAT family *N*-acetyltransferase	3.5	1.7E−33	4.0	5.3E−40
U737_12645	FMN-binding negative transcriptional regulator	4.2	3.7E−45	4.8	8.4E−53
U737_12650	Tautomerase family protein	3.4	7.6E−31	3.2	1.6E−27
U737_12655	DUF1330 domain-containing protein	3.3	3.0E−30	3.2	1.1E−28
U737_12660	CTP synthase	4.6	5.4E−58	4.8	3.7E−61
U737_12665	α/β Hydrolase	4.5	4.9E−50	4.7	3.5E−53
U737_12670	Amidase	3.3	6.8E−29	3.3	3.8E−30
U737_12675	Signal peptidase II	3.2	1.4E−28	3.5	4.7E−33
U737_12680	GFA family protein	3.1	7.9E−26	3.3	6.4E−29
U737_12685	Methyltransferase domain-containing protein	4.1	5.7E−49	4.4	4.2E−53
U737_12690	HAD family hydrolase	6.6	5.3E−86	7.2	2.7E−93
U737_12695	Hypothetical protein	9.4	1.5E−118	9.9	3.4E−123
U737_12700	GNAT family *N*-acetyltransferase	7.6	3.2E−86	8.7	8.2E−99
U737_12705	SAM-dependent methyltransferase	9.0	4.0E−107	9.8	6.4E−116
U737_12710	DUF4260 family protein	7.6	5.6E−88	8.7	4.0E−100
U737_12715	Hypothetical protein	2.9	7.9E−24	3.1	4.4E−28
U737_12720	Cupin domain-containing protein	2.9	4.9E−23	2.5	1.2E−16
U737_12725	DUF4442 domain-containing protein	2.4	5.5E−16	2.6	1.4E−18
U737_12730	Hypothetical protein	1.7	8.5E−06	1.9	1.7E−08
U737_12735	CYTH domain-containing protein	4.5	5.7E−49	4.4	8.9E−47
U737_12740	Transglutaminase family protein	5.1	4.6E−55	5.6	2.5E−62
U737_12745	NAD(P)H-dependent oxidoreductase	6.2	1.4E−68	6.8	1.2E−76

[a]All genes with adjusted *P* values (48) of <0.1 are shown.
[b]GFA, glutathione-dependent formaldehyde-activating enzyme; SAM, *S*-adenosylmethionine; PAP2, phosphatidic acid phosphatase 2; GNAT, Gcn5-related *N*-acetyltransferase; FMN, flavin mononucleotide; HAD, haloacid dehydrogenase.

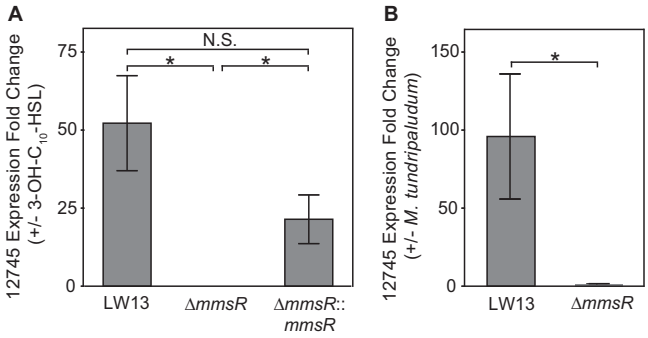

FIG 4 MmsR activation of U737_12745 transcription in response to 3-OH-C_{10}-HSL or coculture with *M. tundripaludum*. Real-time qRT-PCR results showing relative expression of U737_12745, the first ORF in the neighboring gene cluster, for the wild-type LW13, Δ*mmsR*, and complemented Δ*mmsR*::*mmsR* strains in the presence versus the absence of 2 μM 3-OH-C_{10}-HSL (A) or the wild-type LW13 and Δ*mmsR* strains with versus without coculture with *M. tundripaludum* (B). Data are the mean ± standard deviation of three technical replicates and are representative of two independent experiments. *, significantly different (one-tailed homoscedastic *t* test, *P* value of <0.01); N.S., not significant.

first ORF (U737_12745), which was predicted to encode an NAD(P)H-dependent oxidoreductase, was upregulated approximately 6-fold in the presence of acyl-HSL. The results were very similar for comparisons of wild-type LW13 in the presence versus the absence of acyl-HSL or LW13 versus Δ*mmsR* in the presence of acyl-HSL (Table 1).

In order to confirm that MmsR is the cause of the response to the acyl-HSL, we complemented the Δ*mmsR* mutation by inserting *mmsR*, under its native promoter, into a distal site in the genome. This strain (Δ*mmsR*::*mmsR*) regained sensitivity to the acyl-HSL signal, as demonstrated by real-time quantitative reverse transcription-PCR (qRT-PCR) (Fig. 4A). These results confirm that MmsR activates expression of the neighboring gene cluster in the LW13 genome in response to an acyl-HSL signal.

LW13 gene expression is affected during coculture with *M. tundripaludum* in an *mmsR*-dependent manner. Several studies have examined the dynamics of competition between different methane-oxidizing species, including LW13 and *M. tundripaludum*, during growth on methane gas (5, 6). Because these two bacteria were isolated from the same environment (13) and 3-OH-C_{10}-HSL is produced by *M. tundripaludum* and detected by LW13, we tested whether LW13 gene expression was affected during coculture of these two organisms. We isolated RNA from an exponentially growing coculture of these strains and confirmed that U737_12745, the first ORF in the MmsR-regulated cluster, was upregulated compared to a coculture of *M. tundripaludum* and the Δ*mmsR* strain (Fig. 4B).

Researchers previously observed that LW13 outcompetes *M. tundripaludum* in laboratory cocultures (33). We tested whether this result is due to eavesdropping of the *M. tundripaludum* acyl-HSL signal by LW13. However, a planktonic coculture of *M. tundripaludum* and the Δ*mmsR* strain showed no difference in dynamics, compared to a planktonic coculture of *M. tundripaludum* and wild-type LW13 (Fig. S3). This suggests that, under these conditions, gene regulation by MmsR is not the dominant factor in LW13 outcompeting *M. tundripaludum* in laboratory cocultures. Together, these results show that LW13 can use MmsR to alter its gene expression in response to a chemical signal produced by another methane-oxidizing species that may compete for the same ecological niche.

DISCUSSION

We have determined that several species of the methane-oxidizing bacterial genus *Methylomonas*, including strain LW13, possess an orphan acyl-HSL receptor/transcription factor, termed MmsR, that can detect and respond to multiple acyl-HSL signals, including 3-OH-C_{10}-HSL, which is produced by the QS system of an *M. tundripaludum* strain that was isolated from the same environment. In response to a signal, MmsR

activates the transcription of a neighboring gene cluster via an identified binding site.

MmsR shows broader specificity for acyl-HSL signals than does MbaR from *M. tundripaludum* in *E. coli* reporter assays. This promiscuity has been observed for other orphan LuxR-type receptor/transcription factors as well, including QscR from *Pseudomonas aeruginosa*, which responds to both 3-oxo-C_{12}-HSL made by *P. aeruginosa* and other signals that presumably come from external environments (34). This makes intuitive sense, because orphans like MmsR do not have a cognate signal synthase, unlike MbaR with the 3-OH-C_{10}-HSL-producing MbaI. It may also point to a different role for these orphans, related to detecting the presence of other species rather than detecting population density. There are other species in the same environment that also produce acyl-HSLs that would activate MmsR. For example, some *Burkholderia* and *Pseudomonas* species are known to produce 3-OH-C_{10}-HSL (35, 36), and these genera have been detected in the same samples of Lake Washington sediment (5, 6, 9).

The phenotypic response of LW13 to acyl-HSL signal detection by MmsR is still under investigation. The MmsR-activated gene cluster contains several genes that are conserved in all *Methylomonas* strains containing *mmsR*, including genes predicted to encode an NAD(P)H-dependent oxidoreductase, a transglutaminase, and a phosphatase (see Fig. S2 in the supplemental material). The role of this gene cluster is currently unknown, and it is not predicted to produce a specialized metabolite (37).

There are also notable differences in the LW13 cluster, compared to the gene clusters in other *Methylomonas* species. For example, in all other strains the NAD(P)H-dependent oxidoreductase gene is fused with the downstream transglutaminase gene, while in LW13 these are separate ORFs. Additionally, a predicted shikimate dehydrogenase gene that is conserved in all of the other *Methylomonas* clusters is truncated in LW13 (Fig. S2). This raises the possibility that the MmsR-regulated cluster in LW13 is not functional, and future studies will need to be performed on other *Methylomonas* strains in order to determine the function of this cluster in response to acyl-HSL signals.

We investigated whether MmsR plays a role in interactions between LW13 and *M. tundripaludum* in laboratory cocultures. First, we demonstrated that coculturing *M. tundripaludum* with LW13 caused expression of the MmsR-regulated gene cluster, showing that interspecies chemical communication occurs under these conditions. Next, we assessed the dynamics of competition between *M. tundripaludum* and an LW13 Δ*mmsR* mutant. The Δ*mmsR* strain still outcompeted *M. tundripaludum* in a planktonic coculture (Fig. S3), showing that acyl-HSL eavesdropping is not the dominant reason behind LW13 outcompeting *M. tundripaludum* under these laboratory conditions.

These pairwise competitions may not reflect what occurs in the environment; therefore, we do not know the role of this communication system in a natural setting. When lake sediment known to contain both *Methylomonas* species and *M. tundripaludum* is enriched on methane under some conditions, it is *M. tundripaludum* that eventually outcompetes *Methylomonas* species (5, 6, 33). Further studies will be needed to determine the role of this newly identified interspecies chemical communication system in this ecologically significant group of bacteria.

MATERIALS AND METHODS

Plasmid construction. Plasmids used in this study are listed in Table 2, and primers used in this study are listed in Table 3. All plasmids were constructed using Gibson assembly (38), with the exception of the reporter vectors pAWP169 and pAWP179. pAWP169 was constructed by amplifying the sequence containing the putative *lux* box from −400 bp to +21 bp of the translation start site of U737_12745 from LW13 genomic DNA. This sequence was inserted into the promoter probe plasmid pPROBE-GFP[LVA] (39) using the SacI and EcoRI restriction sites. pAWP179 was constructed using the same backbone, promoter, and restriction sites, but the 421-bp promoter sequence contains a CT-to-TA mutation in the MmsR binding sequence (Fig. 2A) and was ordered as a gBlock from Integrated DNA Technologies.

Strain growth. Strains used in this study are listed in Table 2. *E. coli* strains were grown in Luria-Bertani (LB) medium at 37°C. *M. tundripaludum* 21/22 and *Methylomonas* sp. strain LW13 were cultured in an atmosphere of 25% methane in air. For routine culturing, plates were incubated at room temperature in sealed jars (Oxoid Ltd.), while liquid cultures were grown at 18°C in 250-ml glass serum bottles (Kimble Chase) or tubes (18 by 150 mm; Bellco Glass) sealed with rubber stoppers and aluminum

TABLE 2 Strains and plasmids used in this study

Strain or plasmid	Description[a]	Source or reference
Strains		
E. coli TOP10	F⁻ *mcrA* Δ(*mrr-hsdRMS-mcrBC*) φ80*lacZ*ΔM15 Δ*lacX74 recA1 araD139* Δ(*ara leu*) 7697 *galU galK rpsL* (Sm^r) *endA1 nupG*	Invitrogen
E. coli S17-1 λpir	Donor strain; Tp^r Sm^r *recA thi pro hsd*(r⁻m⁺) RP4-2-Tc::Mu::Km Tn*7* λ*pir*	41
mbaR E. coli reporter strain P_{mbaI}-*gfp*	Acyl-HSL reporter strain; *E. coli* TOP10 with pAWP112 and pAWP113	12
mmsR E. coli reporter strain P_{12745}-*gfp*	Acyl-HSL reporter strain; *E. coli* TOP10 with pAWP134 and pAWP169	This study
mmsR E. coli reporter strain with mutated *lux* box, $P_{12745mut}$-*gfp*	Acyl-HSL reporter strain; *E. coli* TOP10 with pAWP134 and pAWP179	This study
M. tundripaludum strain 21/22	Aerobic methane-oxidizing bacterium isolated from sediment from Lake Washington (Seattle, WA, USA)	13
M. tundripaludum strain 21/22 Δ*mbaI* strain	Strain containing unmarked deletion of *luxI*-type acyl-HSL synthase gene *mbaI* (T451DRAFT_0796)	12
Methylomonas sp. strain LW13	Aerobic methane-oxidizing bacterium isolated from sediment from Lake Washington	13
Methylomonas sp. strain LW13 Δ*mmsR* strain	Strain containing unmarked deletion of orphan *luxR*-type transcription factor gene *mmsR* (U737_12750)	This study
Methylomonas sp. strain LW13 Δ*mmsR*::*mmsR* strain	Δ*mmsR* with *mmsR* under its native promoter (400-bp upstream sequence) inserted between U737_06900 and U737_06905	This study
Plasmids		
pAWP112	pPROBE-gfp[LVA] (39) containing *gfp* driven by the P_{mbaI} promoter	12
pAWP113	pACYC184 (49) expressing *mbaR* under its native promoter (400-bp upstream sequence)	12
pAWP134	pACYC184 (49) expressing *mmsR* under its native promoter (400-bp upstream sequence)	This study
pAWP136	pCM433kanT (42) containing flanks to create clean deletion of *mmsR*	This study
pAWP169	pPROBE-gfp[LVA] (39) containing *gfp* driven by −400 bp to +21 bp of the translational start site of U737_12745	This study
pAWP179	pAWP169 with mutation of CT to TA in MmsR binding site (AGCTGTC AATATTGACAGTT to AGTAGTCAATATTGACAGTT) (see Fig. 2)	This study
pAWP195	Insertion vector (site between U737_06900 and U737_06905)	This study
pAWP197	pAWP195 containing *mmsR* under its native promoter (400-bp upstream sequence) for insertion between U737_06900 and U737_06905	This study

[a]Sm^r, streptomycin resistance; Tp^r, trimethoprim resistance.

seals (Wheaton), with shaking at 200 rpm. Cultures were grown in nitrate mineral salts (NMS) medium (40) containing 0.2 g/liter $MgSO_4 \cdot 7H_2O$, 0.2 g/liter $CaCl_2 \cdot 6H_2O$, 1 g/liter KNO_3, and 30 μM $LaCl_3$, as well as 1× trace elements (500× trace elements contains 1.0 g/liter Na_2-EDTA, 2.0 g/liter $FeSO_4 \cdot 7H_2O$, 0.8 g/liter $ZnSO_4 \cdot 7H_2O$, 0.03 g/liter $MnCl_2 \cdot 4H_2O$, 0.03 g/liter H_3BO_3, 0.2 g/liter $CoCl_2 \cdot 6H_2O$, 0.6 g/liter $CuCl_2 \cdot 2H_2O$, 0.02 g/liter $NiCl_2 \cdot 6H_2O$, and 0.05 g/liter $Na_2MoO \cdot 2H_2O$). A final concentration of 5.8 mM phosphate buffer (pH 6.8) was added immediately before use.

Genetic manipulation. Genetic manipulation of LW13 was carried out at 30°C. Plasmids were conjugated into *Methylomonas* sp. strain LW13 using the *E. coli* donor strain S17-1 (41), as described previously (42). For conjugation, LW13 biomass was spread on an NMS plate and grown under methane. The next day, an equal volume of donor biomass containing the plasmid of interest was added and the mixture was grown under methane for 2 additional days. Successful integrants (single crossovers) were selected on NMS plates containing kanamycin (50 μg/ml) and then were used to inoculate a 5-ml NMS liquid culture containing no antibiotics that was grown under methane. After one passage, this culture was plated on an NMS plate containing 1% (m/v) sucrose for counterselection, and the resulting colonies were screened for double crossovers by kanamycin sensitivity and colony PCR.

Genome resequencing, assembly, and annotation. Short-read data for LW13 (genome identification no. 2561511042) were downloaded from the Joint Genome Institute Integrated Microbial Genomes and Microbiomes (JGI IMG/M) data management system (43). The paired-end reads were split into separate forward and reverse read files. Long reads were generated from a separate DNA isolation, using the MasterPure complete DNA and RNA purification kit (Lucigen), from 500 ml of stationary-phase culture. The sequencing library was prepared using the Oxford Nanopore rapid sequencing kit (product no. SQK-RAD004) and immediately loaded onto an Oxford Nanopore MinION long-read sequencer (see the supplemental material). Bases were called from the raw data using MinKNOW v1.15.1. Adapter sequences were removed using porechop v.0.2.3 with the command "porechop -i long_reads.fastq -o trimmed_long_reads.fastq -t 10."

Both short and long reads were included in a hybrid assembly using Unicycler v0.4.7 (44), with the command "python unicycler-runner.py -1 short_forward.fastq -2 short_reverse.fastq -l trimmed_long_reads.fastq -o Assembly," resulting in a single 5,233,523-bp circular contig (see Fig. S1 in the supple-

TABLE 3 Cloning primers used in this study

Primer name	Sequence (5′ to 3′)[a]	Description
AP186_pCM433kanT_fwd1	ATGTGCAGGTTGTCGGTGTC	For amplification of pCM433kanT (42) backbone
AP187_pCM433kanT_rev1	TGGTAACTGTCAGACCAAGTTTACTC	
AP410_113V_fwd1	ACTATGACTGAGAGTCAACG	For amplification of pACYC184 (49) vector backbone
AP411_113V_rev1	TATGCGACTCCTGCATTAGG	
AP517_134I_fwd1	CCTAATGCAGGAGTCGCATATAAGGGCAAGTCGCCAAGCC	For amplification of *mmsR* under its native promoter (400-bp upstream sequence) for insertion into pACYC184
AP518_1341_rev1	CGTTGACTCTCAGTCATAGTTTACAAAAAACCGAGCAGCG	
AP521_136U_fwd1	ATATGAGTAAACTTGGTCTGACAGTTACCAAGAGTATTTCCGGCATAGCC	For amplification of flanks to create Δ*mmsR* clean deletion with pCM433kanT (42)
AP522_136U_rev1	CCAGTTGGATGGTTGGGGTTTACCGTCGTTAGAAC	
AP523_136D_fwd1	AACGACGGTAAACCCCAACCATCCAACTGGAGTCC	
AP524_136D_rev1	CGTGCATCACGACACCGACAACCTGCACATTTTCGAGTCGGACATTTGGC	
AP658_169I_SacI_Fwd1	GGTGGTGAGCTCCGCCAACCTAAGTCCATAGGCA	For amplification of −400 bp to +21 bp of translational start site of U737_12745 for insertion into pPROBE-gfp[LVA] (39) promoter probe vector
AP659_169I_EcoRI_Rev1	GGTGGTGAATTCGGATAAAGCCAGTATTTTCATTGC	
AP758_195I_fwd1	ATATGAGTAAACTTGGTCTGACAGTTACCAACCATTAACGGCGAAGTCAG	For amplification of insertion region between U737_06900 and U737_06905 in LW13 genome; region was added to pCM433kanT (42) opened with AP186 and AP187 to create insertion vector pAWP195
AP759_195I_rev1	CGTGCATCACGACACCGACAACCTGCACATAATTTCTCGGCGATTGTCAG	
AP764_197V_fwd1	TACGCGATACAGCGGGCTTT	For addition of *mmsR* under its native promoter (400-bp upstream sequence) to insertion vector pAWP195
AP765_197V_rev1	CCGAGTACCACTACAGAGCT	
AP766_197I_fwd1	ATTAGTTGTAAGCTCTGTAGTGGTACTCGGTAAGGGCAAGTCGCCAAGCC	
AP767_197I_rev1	CAGGCAAAAAAAAGCCCGCTGTATCGCGTATTACAAAAAACCGAGCAGCG	

[a]Homology regions used for Gibson assembly and restriction enzyme sites are underlined.

mental material). Final annotations were created through submission to the National Center for Biotechnology Information whole-genome sequencing (WGS) submission portal.

RNA extraction, transcriptome sequencing, and data analysis. Growing cultures of *Methylomonas* sp. strain LW13 were subdiluted to an optical density at 600 nm (OD_{600}) of 0.01 and added to bottles containing dried 3-OH-C_{10}-HSL (or solvent control), resulting in a final concentration of 2 μM signal. RNA was extracted during log phase (OD_{600} of 0.4 to 0.6). Briefly, cultures were chilled on ice and then centrifuged at 5,000 rpm for 15 min at 4°C. Pellets were subsequently flash frozen in liquid nitrogen and stored at −80°C until further processing. Cell pellets were lysed by bead beating with 0.1-mm zirconia-silica beads (Biospec Products) in 1 ml TRIzol (Thermo Fisher Scientific). The lysate was then separated according to the TRIzol instructions; subsequently, 1.5 volumes of 100% ethanol was added to the aqueous phase of the extract, which was then used as the input for an RNEasy RNA isolation kit (Qiagen). The resulting eluate was then digested using Ambion DNase I (Thermo Fisher Scientific) for 30 min at 37°C before being repurified via an RNEasy RNA isolation kit with the addition of an on-column DNase (Qiagen) digestion step for 15 min at room temperature. The resulting purified RNA was checked for DNA contamination by PCR using the degenerate 16S primers 27F and 1492R.

cDNA library preparation and RNA sequencing were performed by GENEWIZ using Illumina HiSeq paired-ended reads (2 by 150 bp). The raw reads from the sequencing facility were aligned to the newly assembled *Methylomonas* sp. strain LW13 genome. Alignment was performed using BWA v0.7.12-r1044, using the BWA-MEM algorithm and default parameters (45). The alignments were postprocessed into sorted BAM files with SAMTools v1.2-232-g87cdc4a (46). Reads were attributed to ORFs using the htseq-count tool from HTSeq framework v0.6.1p1, in the intersection-nonempty mode (47). Differential abundance analysis was performed with DESeq2 1.2.10 (48) using R 3.3.0.

Acyl-HSL response *E. coli* reporter assay. Responses to acyl-HSLs signals were detected as described previously (12, 32). Briefly, overnight cultures of *E. coli* reporter strains containing plasmids pAWP112 and pAWP113 (P_{mbal}-*gfp*), pAWP134 and pAWP169 (P_{12745}-*gfp*), or pAWP134 and pAWP179 ($P_{12745mut}$-*gfp*) were subcultured to an OD_{600} of 0.1 in LB medium with kanamycin (50 μg/ml) and chloramphenicol (35 μg/ml). Subsequently, 500 μl was added to 1.5-ml tubes containing dried signal, and the tubes were shaken at 37°C for 4 h. Cultures were then pelleted and resuspended in 500 μl of 50 mM Tris (pH 7.5), and 100 μl was measured for GFP fluorescence (excitation, 485 nm; emission, 510 nm) in a 96-well plate (Nunc black optical bottom) with a plate reader (Tecan Infinite F500). The signals *N*-3-hydroxydecanoyl-L-homoserine lactone (3-OH-C_{10}-HSL), *N*-3-hydroxyoctanoyl-L-homoserine lactone (3-OH-C_8-HSL), and *N*-decanoyl-L-homoserine lactone (C_{10}-HSL) were purchased from Cayman Chemical. The signals *N*-3-oxodecanoyl-L-homoserine lactone (3-oxo-C_{10}-HSL) and *N*-3-hydroxydodecanoyl-DL-homoserine lactone (3-OH-C_{12}-HSL) were purchased from Sigma-Aldrich. When an ethyl acetate extract of methanotroph supernatant was used, it contained the equivalent of 100 μl of supernatant.

Real-time qRT-PCR. One microgram of RNA, isolated as described above, was reverse transcribed using the SensiFAST cDNA synthesis kit (Bioline). PCR mixtures were prepared using the SensiFAST SYBR No-ROX kit (Bioline), containing 400 nM primers and 4 μl undiluted cDNA in a total volume of 10 μl. Reactions were performed on a PTC-200 thermal cycler with a Chromo4 continuous fluorescence detector (MJ Research), and threshold cycle (C_T) values were calculated using Opticon Monitor v3.1.32, at 1 standard deviation from baseline. All gene C_T values were normalized to LW13 *recA* (U737_07580) C_T values, and primers used for all reactions are listed in Table 4.

TABLE 4 Real-time quantitative PCR primers used in this study

Primer name	Sequence (5′ to 3′)	Target
AP692_FMNred_fwd1	GCGGCATCAATCACTTTACCG	NAD(P)H-dependent oxidoreductase gene U737_12745
AP693_FMNred_rev1	ATGGTTTCATCGCCGGTGAT	
AP854_LW13-recA_qPCR_fwd1	AAGTCCGGTTCCTGGTATGC	*recA* gene U737_07580
AP855_LW13-recA_qPCR_rev1	CGTCGTCGTCTTCACTGAC	
21/22 MtYF	GATAGTCGCCGGCTCAGGACGCAT	*M. tundripaludum* formaldehyde oxidation gene *orfY* (T451DRAFT_3399); for coculture species abundance quantification
21/22 MtYR	CTACAGCAGGCGCTAAATCTTGTTC	
LW13YF	CCTAAGTGTTTGTTAGTGATTGCC	LW13 formaldehyde oxidation gene *orfY* (U737_14825); for coculture species abundance quantification
LW13YR	CCAATGACGGCACCTGATATGTAT	

Coculture growth. For qRT-PCR assays, exponentially growing cultures of *M. tundripaludum* 21/22 and LW13 were each subdiluted to an OD_{600} of 0.01 in a 50-ml volume to initiate cocultures. Cocultures were grown to log phase (OD_{600} of 0.4 to 0.6), and RNA was then isolated and analyzed by qRT-PCR as described above.

Coculture competition assays were performed as described previously (33). All cocultures were grown in an atmosphere of 25% methane in air. Briefly, a 1:1 ratio of exponentially growing cultures of *M. tundripaludum* and wild-type or Δ*mmsR* LW13 strains were added to a total OD_{600} of ~0.1 in a 50-ml volume and were grown to an OD_{600} of ~0.6 before subdilution to 0.1 again in order to maintain exponential growth. This process was repeated for a total of 8 days, with samples taken every 2 days for determination of species abundance. DNA was isolated from coculture samples using a GeneJET genomic DNA purification kit (Thermo Fisher Scientific), and species abundance was determined by real-time quantitative PCR as described above, using species-specific primers (Table 4). Bacterial abundances were calculated from C_T values by comparison to a standard curve.

Accession number(s). The new LW13 genome is available at GenBank under accession no. CP033381. The transcriptome sequencing data have been submitted to the Gene Expression Omnibus (GEO) database under accession no. GSE122293.

SUPPLEMENTAL MATERIAL

Supplemental material for this article may be found at https://doi.org/10.1128/AEM.02702-18.

SUPPLEMENTAL FILE 1, PDF file, 0.9 MB.

ACKNOWLEDGMENTS

This work was supported by grants from the U.S. National Institutes of Health (grant K99 GM118762 to A.W.P. and grant R01 GM059026 to E.P.G.) and by the U.S. Department of Energy, Office of Science, Office of Biological and Environmental Research (award DE-SC-0010556 to M.E.L.). M.W.P. was supported by a postdoctoral fellowship from the Mistletoe Foundation.

We thank A. H. S. Jmaileh and N. Ahmed for assistance with preliminary experiments, N. Smalley for assistance with RNA quality assessment, and members of the Lidstrom and Greenberg laboratory for helpful discussions.

A.W.P., A.L.S., E.P.G., and M.E.L. designed the experiments, A.W.P., D.L., and Z.Y. performed experiments, M.W.P. performed genome resequencing, assembly, and annotation and helped with RNA sequencing analysis, and A.W.P., A.L.S., E.P.G., and M.E.L. wrote and edited the manuscript; all authors have read and approved the final version.

REFERENCES

1. Nisbet EG, Dlugokencky EJ, Bousquet P. 2014. Atmospheric science: methane on the rise–again. Science 343:493–495. https://doi.org/10.1126/science.1247828.
2. Singh BK, Bardgett RD, Smith P, Reay DS. 2010. Microorganisms and climate change: terrestrial feedbacks and mitigation options. Nat Rev Microbiol 8:779–790. https://doi.org/10.1038/nrmicro2439.
3. Auman AJ, Stolyar S, Costello AM, Lidstrom ME. 2000. Molecular characterization of methanotrophic isolates from freshwater lake sediment. Appl Environ Microbiol 66:5259–5266. https://doi.org/10.1128/AEM.66.12.5259-5266.2000.
4. Kalyuzhnaya MG, Lapidus A, Ivanova N, Copeland AC, McHardy AC, Szeto E, Salamov A, Grigoriev IV, Suciu D, Levine SR, Markowitz VM, Rigoutsos I, Tringe SG, Bruce DC, Richardson PM, Lidstrom ME, Chistoserdova L. 2008. High-resolution metagenomics targets specific functional types in complex microbial communities. Nat Biotechnol 26:1029–1034. https://doi.org/10.1038/nbt.1488.
5. Oshkin IY, Beck DA, Lamb AE, Tchesnokova V, Benuska G, McTaggart TL, Kalyuzhnaya MG, Dedysh SN, Lidstrom ME, Chistoserdova L. 2015. Methane-fed microbial microcosms show differential community dynamics and pinpoint taxa involved in communal response. ISME J 9:1119–1129. https://doi.org/10.1038/ismej.2014.203.
6. Hernandez ME, Beck DAC, Lidstrom ME, Chistoserdova L. 2015. Oxygen availability is a major factor in determining the composition of microbial communities involved in methane oxidation. PeerJ 3:e801. https://doi.org/10.7717/peerj.801.
7. Yu Z, Chistoserdova L. 2017. Communal metabolism of methane and the rare earth element switch. J Bacteriol 199:e00328-17. https://doi.org/10.1128/JB.00328-17.

8. Yu Z, Beck DAC, Chistoserdova L. 2017. Natural selection in synthetic communities highlights the roles of *Methylococcaceae* and *Methylophilaceae* and suggests differential roles for alternative methanol dehydrogenases in methane consumption. Front Microbiol 8:2392. https://doi.org/10.3389/fmicb.2017.02392.
9. Beck DAC, Kalyuzhnaya MG, Malfatti S, Tringe SG, Glavina Del Rio T, Ivanova N, Lidstrom ME, Chistoserdova L. 2013. A metagenomic insight into freshwater methane-utilizing communities and evidence for cooperation between the *Methylococcaceae* and the *Methylophilaceae*. PeerJ 1:e23. https://doi.org/10.7717/peerj.23.
10. van der Ha D, Vanwonterghem I, Hoefman S, De Vos P, Boon N. 2013. Selection of associated heterotrophs by methane-oxidizing bacteria at different copper concentrations. Antonie Van Leeuwenhoek 103:527–537. https://doi.org/10.1007/s10482-012-9835-7.
11. Krause SMB, Johnson T, Samadhi Karunaratne Y, Fu Y, Beck DAC, Chistoserdova L, Lidstrom ME. 2017. Lanthanide-dependent cross-feeding of methane-derived carbon is linked by microbial community interactions. Proc Natl Acad Sci U S A 114:358–363. https://doi.org/10.1073/pnas.1619871114.
12. Puri AW, Schaefer AL, Fu Y, Beck DAC, Greenberg EP, Lidstrom ME. 2017. Quorum sensing in a methane-oxidizing bacterium. J Bacteriol 199:e00773-16. https://doi.org/10.1128/JB.00773-16.
13. Kalyuzhnaya MG, Lamb AE, McTaggart TL, Oshkin IY, Shapiro N, Woyke T, Chistoserdova L. 2015. Draft genome sequences of gammaproteobacterial methanotrophs isolated from Lake Washington sediment. Genome Announc 3:e00103-15. https://doi.org/10.1128/genomeA.00103-15.
14. Papenfort K, Bassler BL. 2016. Quorum sensing signal-response systems in Gram-negative bacteria. Nat Rev Microbiol 14:576–588. https://doi.org/10.1038/nrmicro.2016.89.
15. Whiteley M, Diggle SP, Greenberg EP. 2017. Progress in and promise of bacterial quorum sensing research. Nature 551:313–320. https://doi.org/10.1038/nature24624.
16. Puri AW, Mevers E, Ramadhar TR, Petras D, Liu D, Piel J, Dorrestein PC, Greenberg EP, Lidstrom ME, Clardy J. 2018. Tundrenone: an atypical secondary metabolite from bacteria with highly restricted primary metabolism. J Am Chem Soc 140:2002–2006. https://doi.org/10.1021/jacs.7b12240.
17. Patankar AV, González JE. 2009. Orphan LuxR regulators of quorum sensing. FEMS Microbiol Rev 33:739–756. https://doi.org/10.1111/j.1574-6976.2009.00163.x.
18. Subramoni S, Venturi V. 2009. LuxR-family 'solos': bachelor sensors/regulators of signalling molecules. Microbiology 155:1377–1385. https://doi.org/10.1099/mic.0.026849-0.
19. Ahmer BMM. 2004. Cell-to-cell signalling in *Escherichia coli* and *Salmonella enterica*. Mol Microbiol 52:933–945. https://doi.org/10.1111/j.1365-2958.2004.04054.x.
20. Chugani SA, Whiteley M, Lee KM, D'Argenio D, Manoil C, Greenberg EP. 2001. QscR, a modulator of quorum-sensing signal synthesis and virulence in *Pseudomonas aeruginosa*. Proc Natl Acad Sci U S A 98:2752–2757. https://doi.org/10.1073/pnas.051624298.
21. Lequette Y, Lee J-H, Ledgham F, Lazdunski A, Greenberg EP. 2006. A distinct QscR regulon in the *Pseudomonas aeruginosa* quorum-sensing circuit. J Bacteriol 188:3365–3370. https://doi.org/10.1128/JB.188.9.3365-3370.2006.
22. Hudaiberdiev S, Choudhary KS, Vera Alvarez R, Gelencsér Z, Ligeti B, Lamba D, Pongor S. 2015. Census of solo LuxR genes in prokaryotic genomes. Front Cell Infect Microbiol 5:20. https://doi.org/10.3389/fcimb.2015.00020.
23. Subramoni S, Florez Salcedo DV, Suarez-Moreno ZR. 2015. A bioinformatic survey of distribution, conservation, and probable functions of LuxR solo regulators in bacteria. Front Cell Infect Microbiol 5:16. https://doi.org/10.3389/fcimb.2015.00016.
24. Schaefer AL, Lappala CR, Morlen RP, Pelletier DA, Lu T-YS, Lankford PK, Harwood CS, Greenberg EP. 2013. LuxR- and LuxI-type quorum-sensing circuits are prevalent in members of the *Populus deltoides* microbiome. Appl Environ Microbiol 79:5745–5752. https://doi.org/10.1128/AEM.01417-13.
25. Beck DAC, McTaggart TL, Setboonsarng U, Vorobev A, Goodwin L, Shapiro N, Woyke T, Kalyuzhnaya MG, Lidstrom ME, Chistoserdova L. 2015. Multiphyletic origins of methylotrophy in *Alphaproteobacteria*, exemplified by comparative genomics of Lake Washington isolates. Environ Microbiol 17:547–554. https://doi.org/10.1111/1462-2920.12736.
26. Whitehead NA, Barnard AML, Slater H, Simpson NJL, Salmond GPC. 2001. Quorum-sensing in Gram-negative bacteria. FEMS Microbiol Rev 25:365–404. https://doi.org/10.1111/j.1574-6976.2001.tb00583.x.
27. Zhang R, Pappas KM, Pappas T, Brace JL, Miller PC, Oulmassov T, Molyneaux JM, Anderson JC, Bashkin JK, Winans SC, Joachimiak A. 2002. Structure of a bacterial quorum-sensing transcription factor complexed with pheromone and DNA. Nature 417:971–974. https://doi.org/10.1038/nature00833.
28. Heylen K, De Vos P, Vekeman B. 2016. Draft genome sequences of eight obligate methane oxidizers occupying distinct niches based on their nitrogen metabolism. Genome Announc 4:e00421-16. https://doi.org/10.1128/genomeA.00421-16.
29. Orata FD, Kits KD, Stein LY. 2018. Complete genome sequence of *Methylomonas denitrificans* strain FJG1, an obligate aerobic methanotroph that can couple methane oxidation with denitrification. Genome Announc 6:e00276-18. https://doi.org/10.1128/genomeA.00276-18.
30. Egland KA, Greenberg EP. 1999. Quorum sensing in *Vibrio fischeri*: elements of the *luxI* promoter. Mol Microbiol 31:1197–1204. https://doi.org/10.1046/j.1365-2958.1999.01261.x.
31. Antunes LCM, Ferreira RBR, Lostroh CP, Greenberg EP. 2008. A mutational analysis defines *Vibrio fischeri* LuxR binding sites. J Bacteriol 190:4392–4397. https://doi.org/10.1128/JB.01443-07.
32. Antunes LCM, Schaefer AL, Ferreira RBR, Qin N, Stevens AM, Ruby EG, Greenberg EP. 2007. Transcriptome analysis of the *Vibrio fischeri* LuxR-LuxI regulon. J Bacteriol 189:8387–8391. https://doi.org/10.1128/JB.00736-07.
33. Yu Z, Krause SMB, Beck DAC, Chistoserdova L. 2016. A synthetic ecology perspective: how well does behavior of model organisms in the laboratory predict microbial activities in natural habitats? Front Microbiol 7:946. https://doi.org/10.3389/fmicb.2016.00946.
34. Lee J-H, Lequette Y, Greenberg EP. 2006. Activity of purified QscR, a *Pseudomonas aeruginosa* orphan quorum-sensing transcription factor. Mol Microbiol 59:602–609. https://doi.org/10.1111/j.1365-2958.2005.04960.x.
35. Cha C, Gao P, Chen Y-C, Shaw PD, Farrand SK. 1998. Production of acyl-homoserine lactone quorum-sensing signals by Gram-negative plant-associated bacteria. Mol Plant Microbe Interact 11:1119–1129. https://doi.org/10.1094/MPMI.1998.11.11.1119.
36. Duerkop BA, Varga J, Chandler JR, Peterson SB, Herman JP, Churchill MEA, Parsek MR, Nierman WC, Greenberg EP. 2009. Quorum-sensing control of antibiotic synthesis in *Burkholderia thailandensis*. J Bacteriol 191:3909–3918. https://doi.org/10.1128/JB.00200-09.
37. Blin K, Wolf T, Chevrette MG, Lu X, Schwalen CJ, Kautsar SA, Suarez Duran HG, de Los Santos ELC, Kim HU, Nave M, Dickschat JS, Mitchell DA, Shelest E, Breitling R, Takano E, Lee SY, Weber T, Medema MH. 2017. antiSMASH 4.0: improvements in chemistry prediction and gene cluster boundary identification. Nucleic Acids Res 45:W36–W41. https://doi.org/10.1093/nar/gkx319.
38. Gibson DG, Young L, Chuang R-Y, Venter JC, Hutchison CA, Smith HO. 2009. Enzymatic assembly of DNA molecules up to several hundred kilobases. Nat Methods 6:343–345. https://doi.org/10.1038/nmeth.1318.
39. Miller WG, Leveau JH, Lindow SE. 2000. Improved *gfp* and *inaZ* broad-host-range promoter-probe vectors. Mol Plant Microbe Interact 13:1243–1250. https://doi.org/10.1094/MPMI.2000.13.11.1243.
40. Whittenbury R, Phillips KC, Wilkinson JF. 1970. Enrichment, isolation and some properties of methane-utilizing bacteria. J Gen Microbiol 61:205–218. https://doi.org/10.1099/00221287-61-2-205.
41. Simon R, Priefer U, Pühler A. 1983. A broad host range mobilization system for *in vivo* genetic engineering: transposon mutagenesis in Gram negative bacteria. Nat Biotechnol 1:784–791. https://doi.org/10.1038/nbt1183-784.
42. Puri AW, Owen S, Chu F, Chavkin T, Beck DAC, Kalyuzhnaya MG, Lidstrom ME. 2015. Genetic tools for the industrially promising methanotroph *Methylomicrobium buryatense*. Appl Environ Microbiol 81:1775–1781. https://doi.org/10.1128/AEM.03795-14.
43. Chen I-MA, Chu K, Palaniappan K, Pillay M, Ratner A, Huang J, Huntemann M, Varghese N, White JR, Seshadri R, Smirnova T, Kirton E, Jungbluth SP, Woyke T, Eloe-Fadrosh EA, Ivanova NN, Kyrpides NC. 2019. IMG/M v.5.0: an integrated data management and comparative analysis system for microbial genomes and microbiomes. Nucleic Acids Res 47:D666–D677. https://doi.org/10.1093/nar/gky901.
44. Wick RR, Judd LM, Gorrie CL, Holt KE. 2017. Unicycler: resolving bacterial genome assemblies from short and long sequencing reads. PLoS Comput Biol 13:e1005595. https://doi.org/10.1371/journal.pcbi.1005595.
45. Li H, Durbin R. 2010. Fast and accurate long-read alignment with Burrows-Wheeler transform. Bioinformatics 26:589–595. https://doi.org/10.1093/bioinformatics/btp698.

46. Li H, Handsaker B, Wysoker A, Fennell T, Ruan J, Homer N, Marth G, Abecasis G, Durbin R. 2009. The Sequence Alignment/Map format and SAMtools. Bioinformatics 25:2078–2079. https://doi.org/10.1093/bioinformatics/btp352.
47. Anders S, Pyl PT, Huber W. 2015. HTSeq: a Python framework to work with high-throughput sequencing data. Bioinformatics 31:166–169. https://doi.org/10.1093/bioinformatics/btu638.
48. Anders S, McCarthy DJ, Chen Y, Okoniewski M, Smyth GK, Huber W, Robinson MD. 2013. Count-based differential expression analysis of RNA sequencing data using R and Bioconductor. Nat Protoc 8:1765–1786. https://doi.org/10.1038/nprot.2013.099.
49. Chang AC, Cohen SN. 1978. Construction and characterization of amplifiable multicopy DNA cloning vehicles derived from the P15A cryptic miniplasmid. J Bacteriol 134:1141–1156.